

Anomalous Diffusion of Phospholipids and Cholesterols in a Lipid Bilayer and its Origins

Jae-Hyung Jeon,¹ Hector Martinez-Seara Monne,¹ Matti Javanainen,¹ and Ralf Metzler^{1,2}

¹*Department of Physics, Tampere University of Technology, FI-33101 Tampere, Finland*

²*Institute for Physics and Astronomy, University of Potsdam, D-14476 Potsdam-Golm, Germany*

(Received 23 May 2012; published 31 October 2012)

Combining extensive molecular dynamics simulations of lipid bilayer systems of varying chemical compositions with single-trajectory analyses, we systematically elucidate the stochastic nature of the lipid motion. We observe subdiffusion over more than 4 orders of magnitude in time, clearly stretching into the submicrosecond domain. The lipid motion depends on the lipid chemistry, the lipid phase, and especially the presence of cholesterol. We demonstrate that fractional Langevin equation motion universally describes the lipid motion in all phases, including the gel phase, and in the presence of cholesterol. The results underline the relevance of anomalous diffusion in lipid bilayers and the strong effects of the membrane composition.

DOI: [10.1103/PhysRevLett.109.188103](https://doi.org/10.1103/PhysRevLett.109.188103)

PACS numbers: 87.16.dj, 02.50.-r, 05.40.-a, 87.10.Mn

Recent advances in single molecule spectroscopy unveil anomalous diffusion of microscopic tracers in the crowded environment of living cells, which is starting to reshape our views of molecular cell biology and underlining the role of modern statistical physics [1]. Extensive experimental studies show subdiffusion in terms of the nonlinear scaling in time of the mean squared displacement (MSD) [2]

$$\langle \mathbf{r}^2(t) \rangle \simeq K_\alpha t^\alpha \quad \text{with} \quad 0 < \alpha < 1, \quad (1)$$

where α is the anomalous diffusion exponent and K_α the generalized diffusivity of physical dimension $\text{cm}^2/\text{sec}^\alpha$. Subdiffusion (1) was reported for various microscopic tracers under the densely crowded conditions inside living cells [3–7] and in control experiments [8,9], as well as for proteins in cell membranes [10,11]. These experiments demonstrate the ubiquitous presence of subdiffusion of a large variety of tracers and crowded environments over many orders of magnitude in time, but see Ref. [12]. Subdiffusion alters significantly the diffusion control of biochemical reactions, and its effects are therefore far-reaching for a wide range of molecular cellular processes [13]. While subdiffusion (1) slows down long-distance diffusional exchange and may affect surface-bulk exchange [14], it may indeed be beneficial for local interactions in cells [3,15,16]. Depending on the magnitude of the exponent α , anomalous diffusion may affect the localization of objects such as chromosomes or membrane channels [7,11] and impact the formation and dynamics of membrane domains.

Here we study in detail the diffusive behavior of lipids in bilayer systems through trajectory analysis from extensive molecular dynamics simulations. We find that in all investigated bilayers the lipids exhibit subdiffusion up to a few nanoseconds, before a crossover either to normal diffusion or to persistent anomalous diffusion with a larger exponent. The observed behavior depends strongly on the phospholipid chemistry, their mixture with cholesterol, and the bilayer phase (liquid or gel). Subdiffusion ranges at

least up to several hundreds of nanoseconds in the presence of cholesterols. Our analysis shows that the lipid motion is consistent with viscoelastic subdiffusion driven by correlated Gaussian noise in both liquid and gel phases and, thus, provides a *unified* physical framework for lipid diffusion in membranes.

Subdiffusion (1) is described by several prominent models based on different physical mechanisms [2,17]. In continuous time random walks (CTRWs), jumps are separated by random waiting times τ with heavy-tailed distributions $\psi(\tau) \sim \tau^{-1-\alpha}$ [18]. CTRW motion was identified for microbead motion in reconstituted actin networks [19], lipid granules in cellular cytoplasm [6], and protein channels in plasma membranes [11]. In contrast, fractional Brownian motion (FBM) and the fractional Langevin equation (FLE) produce ergodic subdiffusion (1) with long-ranged anticorrelation ($0 < \alpha < 1$) [20]

$$\langle \Delta \mathbf{r}(t) \cdot \Delta \mathbf{r}(0) \rangle \sim \alpha(\alpha - 1)t^{\alpha-2} \quad (2)$$

of spatial displacements $\Delta \mathbf{r}$. FBM is defined by an overdamped Langevin equation driven by athermal, external Gaussian noise with a power-law correlation. FLE is a generalized Langevin equation driven by the same noise. Because of its memory kernel, the FLE describes thermal motion of a particle in viscoelastic media [21]. While FLE in the overdamped limit produces FBM-like subdiffusive motion, below the momentum relaxation time, FLE motion is ballistic. FBM and FLE motion describe subdiffusion in living cells of mRNA [22], chromosomal loci [4], and lipid granules at longer times [6], as well as the motion of macromolecules in a crowded dextran solution [8]. While sharing the scaling form of the MSD (1), CTRW and FBM or FLE lead to completely different dynamics of diffusion control. Knowledge of the subdiffusion mechanism in membranes is therefore vital to advance our understanding of their physical and biochemical properties.

Lipid bilayers are quasi-two-dimensional, highly packed systems made up of phospholipid molecules, which undergo thermally driven lateral diffusion and thus constantly reorganize the membrane. The lateral MSD of membrane lipids typically spans three distinct regimes: short-time ballistic ($\alpha = 2$), intermediate subdiffusive ($0 < \alpha < 1$), and long-time Brownian motion ($\alpha = 1$) [23,24]. The long-time diffusive motion of various kinds of phospholipid molecules in lipid bilayers has been extensively studied [25,26]. Diffusion of lipids in pure bilayers occurs in both the liquid disordered and the gel phases below the melting temperature, the latter with decreased diffusivity. Moreover, in bilayers mixed with cholesterol, the diffusivity of the lipids tends to decrease with higher cholesterol concentration.

Lipid subdiffusion at shorter time scales is comparatively poorly understood. In the traditional microscopic picture, the lateral movement of lipid molecules is assumed to occur through jumps when sufficient void space is thermally activated at nearest sites [26,27]. Between jumps, the molecule, caged by its neighbors, undergoes rattling motion. This CTRW-type jump-diffusion model has been used to estimate the diffusivities of lipids in the liquid disordered phase and in bilayers containing cholesterol [25,26]. However, atomistic simulations [28] and a quasi-elastic neutron scattering experiment [29] showed that such jumplike displacements rarely occur, and the lipids move concertedly with their neighbors as loosely defined clusters. Moreover, conflicting results were reported on the stochastic nature of the lipid diffusion: References [23,30] demonstrated that the lipid motion is consistent with FLE dynamics, whereas Ref. [31] claimed to observe CTRW-type motion governed by non-Gaussian fluctuations and scale-free rattling dynamics.

Lipid bilayers of 128 phospholipid molecules were studied by molecular dynamics simulations under periodic boundary conditions; for details, see the Supplemental Material [32]. We used three pure single component lipid bilayers composed of DSPC, SOPC, and DOPC phospholipids in the liquid disordered phase [33]. We also studied these systems with additional 32 cholesterol (20% molar concentration) in the liquid ordered phase. A pure membrane of 288 DSPC molecules was also simulated in the gel phase. Figure 1 shows typical snapshots in the three phases. In this work, we focus on the characterization of the lipid diffusion. To that end, we note that during the simulation the centers of mass of the upper and lower lipid layers undergo free, independent translational motion (Fig. S1), as reported previously [31,34]. Free center of mass diffusion causes apparent normal diffusion of individual lipid molecules at longer times, irrespective of their actual diffusion characteristics. To avoid this, we analyze the relative motion $\mathbf{r}(t)$ from the center of mass of lipids and cholesterol. Figures S2, S5, and S11 in the Supplemental Material show sample trajectories.

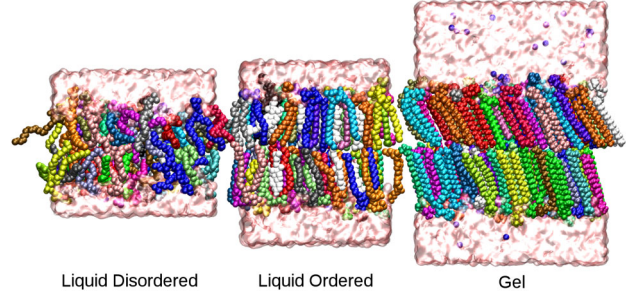


FIG. 1 (color online). Final configurations of simulations of DOPC 338 K (left), DSPC and cholesterol 338 K (middle), and DSPC 310 K (right) in the liquid disordered, liquid ordered, and gel phases, respectively (note the difference in packing states). Each color (gray scale) represents a different phospholipid. Explicit water molecules correspond to the upper and lower transparent coatings. Cholesterol appears in white (middle) and Na^+ and Cl^- ions as blue (darker) spheres (right).

From individual trajectories $\mathbf{r}(t)$, we obtained the time-averaged MSD of lipids typically defined as [3,4,17]

$$\overline{\delta^2(\Delta)} = \frac{1}{T - \Delta} \int_0^{T-\Delta} [\mathbf{r}(t + \Delta) - \mathbf{r}(t)]^2 dt, \quad (3)$$

where Δ is the lag time and T the length of the trajectory (measurement time). Figure 2 shows the mean $\langle \delta^2(\Delta) \rangle$ taken over the trajectories of all phospholipids, for the cases of DSPC, SOPC, and DOPC in the absence and presence of cholesterol. In each case, the result was fitted by $\langle \delta^2(\Delta) \rangle = 4K_\alpha \Delta^\alpha$ at short and long times, respectively. The corresponding diffusion exponents α and diffusivities K_α are summarized in Table I. In Fig. 2, the scaling behaviors for pure DSPC and DOPC at short (solid line) and long (dashed line) times are indicated. In the absence of cholesterol, all three types of lipid molecules show similar

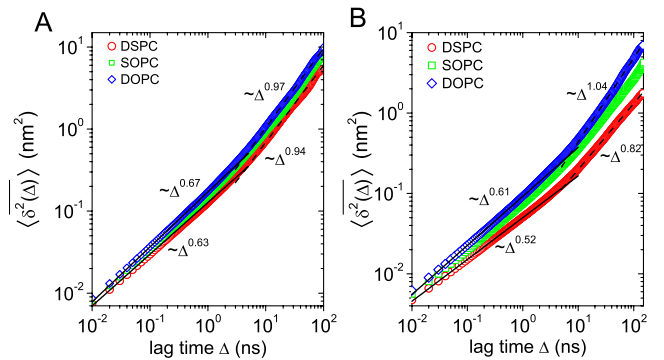


FIG. 2 (color online). Time-averaged MSDs $\langle \delta^2(\Delta) \rangle$ of DSPC, SOPC, and DOPC in liquid phase bilayers. Each curve represents the mean of individual $\delta^2(\Delta)$ taken over all trajectories of 128 phospholipids in the bilayer. (a) Cholesterol-free case. (b) With cholesterol. The results were fitted separately to $\langle \delta^2(\Delta) \rangle = 4K_\alpha \Delta^\alpha$ in the regimes of short [0.01...1 ns] and long times [10, ..., 100 ns]. Fit results for α and K_α are summarized in Table I.

behavior: anomalous diffusion with exponent $\alpha \sim 0.6$ below a crossover time $\tau_c \sim 10$ ns and normal Brownian motion beyond τ_c . The crossover time τ_c roughly corresponds to the diffusion time of a lipid molecule needed to span its nearest-neighbor distance. The structural difference in the tails of the lipids affects somewhat the long-time diffusion, in particular, the values of K_{α_l} .

Figure 2(b) shows that cholesterol significantly affects both the short- and long-time diffusion of the lipids. Especially for saturated DSPC with the smallest cross section area [35], we observe that, below $\tau_c \approx 10$ ns, α decreases to about 0.5 and a new subdiffusion regime emerges with $\alpha \sim 0.8$ up to 100 ns. An additional 1 μ s-long simulation confirms that this new regime above τ_c is in fact a slow transition toward normal diffusion that lasts over hundreds of nanoseconds (Fig. S10). In the displayed time window, the behavior is well fitted by the scaling exponents α_l listed in Table I. For unsaturated DOPC, the effect of cholesterol is small, albeit K_α is significantly reduced, and no second subdiffusion regime occurs.

The observed subdiffusive behavior of lipids is mainly attributed to the unique structural complexity of the lipid molecule. Spherical-shaped hard particle systems cannot have such a long subdiffusion regime and values of α as small as 0.5–0.6 (Fig. S18). To gain additional physical insight into the lipid motion, we now check the detailed stochastic properties of the lipids.

Time-averaged observables obtained from single trajectories provide information on the ergodic properties of a stochastic motion and, thus, about the physical nature of the underlying dynamics. We call a process ergodic when the long-time average of a quantity (e.g., the MSD) equals the corresponding ensemble average [17,36]. For free CTRW subdiffusion [37], $\langle \delta^2(\Delta) \rangle$ grows like Δ , while the ensemble average (1) scales sublinearly [17,38]. Free FLE motion is ergodic [39,40], and $\langle \delta^2(\Delta) \rangle \simeq \Delta^\alpha$. The observation of a sublinear slope in Fig. 2 already indicates that the observed motion is not of CTRW type. This is further confirmed by the independence of δ^2 of the measurement time T [Fig. 3(b)] in contrast to the $T^{\alpha-1}$ scaling of CTRW [17,38]. Figure 3(c) shows the distribution ϕ of trajectory-to-trajectory amplitude variations of $\delta^2(\Delta)$ for the 128 individual molecules of Fig. 3(a), as a function of the

TABLE I. Exponent α and diffusivity K_α ($\text{nm}^2/\text{ns}^\alpha$) of lipids at short (s) and long (l) times. Statistical uncertainty is in parenthesis. Bold: Systems containing 20% cholesterol.

	α_s	K_{α_s}	α_l	K_{α_l}
DSPC	0.63(0.06%)	0.032(2%)	0.94(0.9%)	0.020(5%)
SOPC	0.66(1%)	0.038(2%)	1.00(16%)	0.020(60%)
DOPC	0.67(2%)	0.043(2%)	0.97(13%)	0.028(16%)
DSPC	0.52(1%)	0.013(2%)	0.82(4%)	0.0076(6%)
SOPC	0.58(0.4%)	0.019(0.5%)	0.87(5%)	0.012(4%)
DOPC	0.61(0.5%)	0.023(0.4%)	1.04(22%)	0.0098(41%)

dimensionless variable $\xi = \overline{\delta^2(\Delta)}/\langle \delta^2(\Delta) \rangle$. All curves are centered around the ergodic value $\xi = 1$. The broadening of ϕ with increasing Δ mirrors large fluctuations of δ^2 at long Δ due to insufficient statistics when calculating δ^2 . ϕ also narrows at fixed Δ when T is increased (Fig. S3). These properties demonstrate that the lipid molecules perform ergodic motion different from CTRW.

We obtained the displacement autocorrelation function

$$C_{\delta t}(t) = \langle [\mathbf{r}(t + \delta t) - \mathbf{r}(t)] \cdot [\mathbf{r}(\delta t) - \mathbf{r}(0)] \rangle / \delta t^2 \quad (4)$$

for arbitrary time step δt for several diffusion models in Supplemental Material Sec. III [32]. Normalized, $C_{\delta t}(t)/C_{\delta t}(0)$ is a fit-free function for given δt and α . Figure 3(d) shows $C_{\delta t}(t)/C_{\delta t}(0)$ at $\delta t = 0.2$ ns of DSPC lipids from simulations in the subdiffusion regime, along with theoretical results for CTRW and FLE motion [32]. We find excellent agreement with FLE motion. Here $\alpha = 0.63$ was taken from the TA MSD. The lipid motion is thus anticorrelated, in line with Eq. (2). The behavior in Fig. 3(d) differs distinctly from free CTRW motion [17], where $C_{\delta t}(t) = 0$ for $t > \delta t$ (dashed line). Figure 3(e)

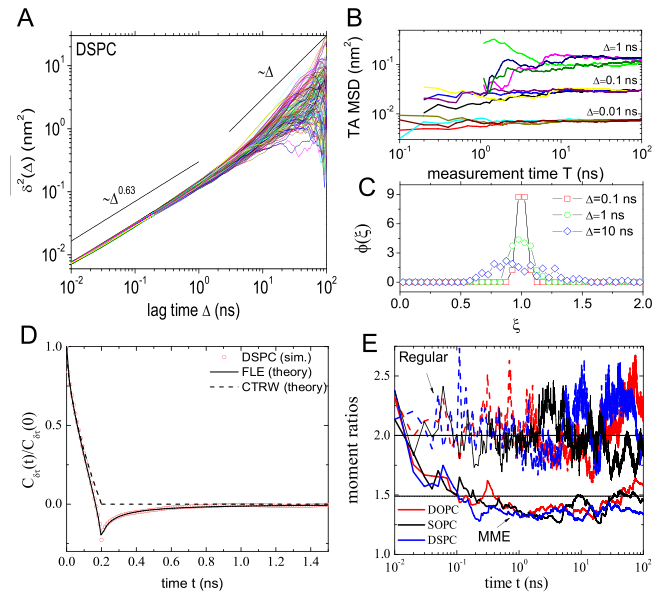


FIG. 3 (color online). Stochastic analysis of DSPC in pure liquid phase bilayer. (a) TA MSD $\delta^2(\Delta)$ of all 128 DSPC molecules. (b) $\delta^2(\Delta)$ versus measurement time T , for $\Delta = 0.01, 0.1, 1$ ns. (c) Normalized scatter distribution $\phi(\xi)$ of $\delta^2(\Delta)$ versus $\xi = \delta^2(\Delta)/\langle \delta^2(\Delta) \rangle$, for $\Delta = 0.1, 1, 10$ ns. (d) Displacement autocorrelation function $C_{\delta t}(t)/C_{\delta t}(0)$ of DSPC lipids, $\delta t = 0.2$ ns. The solid and dotted lines represent the fit-free forms of $C_{\delta t}(t)/C_{\delta t}(0)$ for FLE and CTRW (Supplemental Material [32]), respectively, at $\alpha = 0.63$. (e) Moment ratios $\langle \mathbf{r}^4(t) \rangle / \langle \mathbf{r}^2(t) \rangle^2$ (regular) and $\langle r_{\max}^4(t) \rangle / \langle r_{\max}^2(t) \rangle^2$ [mean maximal excursion] for DSPC, SOPC, and DOPC molecules. The horizontal line at 1.49 distinguishes FLE motion [$\langle r_{\max}^4(t) \rangle / \langle r_{\max}^2(t) \rangle^2 < 1.49$] from CTRW [$\langle r_{\max}^4(t) \rangle / \langle r_{\max}^2(t) \rangle^2 > 1.49$]. The horizontal line at 2 is the expected value of the regular moment ratio for both FLE and CTRW motion.

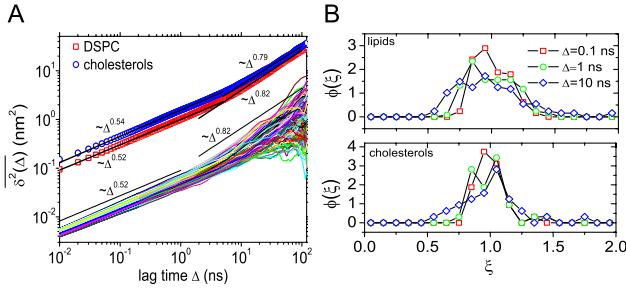


FIG. 4 (color online). DSPC molecules in liquid phase bilayer mixed with cholesterol. (a) $\overline{\delta^2(\Delta)}$ for 128 DSPC molecules (for cholesterol, see Fig. S8). Average TA MSDs $\langle \overline{\delta^2(\Delta)} \rangle$ for cholesterol (blue circle) and DSPCs (red square) are shifted by a factor of 20. (b) Distribution $\phi(\xi)$ for $\overline{\delta^2}$ of DSPCs and cholesterol.

also shows the moment ratios $\langle r^4(t) \rangle / \langle r^2(t) \rangle^2$ and $\langle r_{\max}^4(t) \rangle / \langle r_{\max}^2(t) \rangle^2$, where $r_{\max}(t)$ denotes the maximal distance of a given particle from its initial position reached up to time t [41]. Moment ratios have unique values depending on the stochastic process [41], as summarized in the Supplemental Material [32]. Figure 3(e) shows that $\langle r^4(t) \rangle / \langle r^2(t) \rangle^2$ fluctuates around 2, and $\langle r_{\max}^4(t) \rangle / \langle r_{\max}^2(t) \rangle^2$ decreases from ≈ 2 to stay < 1.49 , as predicted for FLE and violating CTRW.

We conclude that the subdiffusive behavior shown above is robust; all analysis tools convincingly point to FLE motion. Analogous results were obtained for SOPC and DOPC molecules. The results are preserved at varying temperature: Temperature increase leads to an increase of K_{α} only in the Brownian regime (Fig. S4). Consistent with previous studies [28,29], the collective motion of lipids exhibit a flowlike pattern (Fig. S16).

As shown in Fig. 2, the diffusion of the lipid molecules is drastically changed by the presence of cholesterol. Is the stochastic nature also affected by cholesterol? We find that ergodicity of the motion is preserved, while cholesterol significantly affect the distribution $\phi(\xi)$ of $\overline{\delta^2}$. Comparing with the pure bilayer [Fig. 3(c)], with cholesterol $\phi(\xi)$ noticeably broadens [Fig. 4(b)]. Individual lipids thus undergo considerable variations while diffusing in the presence of cholesterol, as seen in Fig. 4(a). Moreover, with cholesterol the displacement autocorrelation $C_{\delta t}(t)$ has a slightly deeper well, consistent with a stronger anti-correlation of the displacement (Fig. S6).

For the motion of the cholesterol molecules themselves, we find that their behavior is almost identical to the lipids', of FLE-type anomalous diffusion. Figure 4(a) compares the TA MSD averaged over all trajectories $\langle \overline{\delta^2(\Delta)} \rangle$ separately for DSPC and cholesterol molecules. While cholesterol universally diffuse faster than the lipids, their scaling behaviors are almost the same. Meanwhile, the scatter distributions of cholesterol are sharper than that of the lipids, implying that cholesterol diffusion is more uniform than that of lipids. This may be related to the fact that at

any moment only some lipids are in direct contact with cholesterol which modifies their behavior from those of the remaining lipids. The displacement autocorrelation of cholesterol is hardly different from that of the lipids in the lipid-cholesterol bilayer (Fig. S9), and the moment ratios agree with FLE motion (Fig. S7).

To obtain a full picture of the diffusive motion in lipid bilayers, we also studied the gel phase. For DSPC molecules we obtain the following: (i) Figure 5(a) shows that $\overline{\delta^2}$ scales with $\alpha_s \approx 0.16$ at short times and is thus remarkably smaller than the value $\alpha_s \approx 0.6$ in the liquid phase. Moreover, in the gel phase the TA MSD remains subdiffusive with $\alpha_l \approx 0.59$ beyond the crossover. (ii) The scatter distribution ϕ of individual $\overline{\delta^2(\Delta)}$ shows that the lipid motion remains ergodic in the gel phase (Fig. S12) [42]. (iii) The results for the gel phase autocorrelation are consistent with FLE motion with exponent $\alpha \approx 0.16$ [Fig. 5(b)], as are the moment ratios (Fig. S13). (iv) Contrasting recent claims [31], the rattling dynamics of lipids is consistent with FLE motion (Figs. S14 and S15).

In summary, we here report extensive molecular dynamics simulations of lipid bilayer systems and the analysis of individual trajectories using stochastic analysis tools. While we find a moderate dependence on the lipid chemistry, the effect of cholesterol is striking. Cholesterol effect more pronounced and persistent subdiffusion. FLE motion is identified as the unifying process for the motion of both phospholipids and cholesterol in liquid and gel phases. Our study thus provides an integral picture of lateral motion of lipids by showing the compatibility of FLE-type stochastic motion of individual molecules and their flowlike collective motion.

Cholesterol significantly affect the phospholipids diffusion via increasing membrane packing and inducing 2D ordering [43] (Fig. 1). α is lowered significantly to ≈ 0.5 below $\tau_c \approx 10$ ns. In agreement, recent experimental and computational studies show that α decreases with increase of the concentration of proteins in the bilayer [44,45]. Interestingly, we observe a pronounced variation between individual lipid's motion, likely due to the asymmetric disturbance caused by cholesterol [43]. While the slowing down of lipid diffusion by cholesterol is known from experiment [26,46] and simulations [34], the dramatic

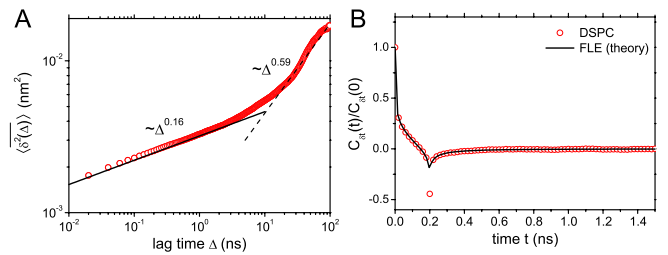


FIG. 5 (color online). DSPC molecules in the gel phase bilayer. (a) $\langle \overline{\delta^2(\Delta)} \rangle$. (b) Displacement autocorrelation $C_{\delta t}(t)/C_{\delta t}(0)$ with $\delta t = 0.2$ ns. Solid line: Theoretical result for FLE with $\alpha = 0.16$.

effects of cholesterol on intermediate-time lipid diffusion have not been reported to our best knowledge.

Given the above results we speculate that in biomembranes, whose complexity is higher than the bilayers studied here (e.g., larger number of lipid moieties, proteins, and higher cholesterol concentration), subdiffusion may range to macroscopic times, thus altering our current view of membrane dynamics. Single particle tracking together with advanced simulations techniques and stochastic analysis tools are promising methods to explore this intriguing possibility.

We thank Otto Pulkkinen and Ilpo Vattulainen for discussions. We acknowledge financial support from the Academy of Finland (FiDiPro scheme) and the CSC-IT Center for Science in Finland for computing resources.

-
- [1] E. Barkai, Y. Garini, and R. Metzler, *Phys. Today* **65**, No. 8, 29 (2012).
- [2] R. Metzler and J. Klafter, *Phys. Rep.* **339**, 1 (2000); *J. Phys. A* **37**, R161 (2004).
- [3] I. Golding and E. C. Cox, *Phys. Rev. Lett.* **96**, 098102 (2006).
- [4] S. Weber, A. J. Spakowitz, and J. A. Theriot, *Phys. Rev. Lett.* **104**, 238102 (2010).
- [5] G. Seisenberger, M. U. Ried, T. Endreß, H. Büning, M. Hallek, and C. Bräuchle, *Science* **294**, 1929 (2001).
- [6] J.-H. Jeon, V. Tejedor, S. Burov, E. Barkai, C. Selhuber-Unkel, K. Berg-Sørensen, L. Oddershede, and R. Metzler, *Phys. Rev. Lett.* **106**, 048103 (2011).
- [7] I. Bronstein, Y. Israel, E. Kepten, S. Mai, Y. Shav-Tal, E. Barkai, and Y. Garini, *Phys. Rev. Lett.* **103**, 018102 (2009).
- [8] J. Szymanski and M. Weiss, *Phys. Rev. Lett.* **103**, 038102 (2009).
- [9] W. Pan, L. Filobelo, N. Pham, O. Galkin, V. Uzunova, and P. Vekilov, *Phys. Rev. Lett.* **102**, 058101 (2009).
- [10] M. Weiss, H. Hashimoto, and T. Nilsson, *Biophys. J.* **84**, 4043 (2003).
- [11] A. V. Weigel, B. Simon, M. M. Tamkun, and D. Krapf, *Proc. Natl. Acad. Sci. U.S.A.* **108**, 6438 (2011).
- [12] Note that there also exist reports on normal diffusion, especially for small tracer particles: J. Elf, G.-W. Li, and X. S. Xie, *Science* **316**, 1191 (2007); J. A. Dix and A. S. Verkman, *Annu. Rev. Biophys.* **37**, 247 (2008).
- [13] A. P. Minton, *J. Cell Sci.* **119**, 2863 (2006); D. Ben-Avraham and S. Havlin, *Diffusion and Reactions in Fractals and Disordered Systems* (Cambridge University Press, Cambridge, England, 2005); E. Abad, S. B. Yuste, and K. Lindenberg, *Phys. Rev. E* **81**, 031115 (2010); D. Froemberg and I. M. Sokolov, *Phys. Rev. Lett.* **100**, 108304 (2008).
- [14] M. A. Lomholt, I. M. Zaid, and R. Metzler, *Phys. Rev. Lett.* **98**, 200603 (2007); I. M. Zaid, M. A. Lomholt, and R. Metzler, *Biophys. J.* **97**, 710 (2009).
- [15] G. Guigas and M. Weiss, *Biophys. J.* **94**, 90 (2008).
- [16] L. E. Sereshki, M. A. Lomholt, and R. Metzler, *Europhys. Lett.* **97**, 20008 (2012).
- [17] S. Burov, J.-H. Jeon, R. Metzler, and E. Barkai, *Phys. Chem. Chem. Phys.* **13**, 1800 (2011); I. M. Sokolov, *Soft Matter* **8**, 9043 (2012).
- [18] H. Scher and E. W. Montroll, *Phys. Rev. B* **12**, 2455 (1975).
- [19] I. Y. Wong, M. L. Gardel, D. R. Reichman, E. R. Weeks, M. T. Valentine, A. R. Bausch, and D. A. Weitz, *Phys. Rev. Lett.* **92**, 178101 (2004).
- [20] E. Lutz, *Phys. Rev. E* **64**, 051106 (2001).
- [21] I. Goychuk, *Adv. Chem. Phys.* **150**, 187 (2012).
- [22] M. Magdziarz, A. Weron, and K. Burnecki, *Phys. Rev. Lett.* **103**, 180602 (2009).
- [23] E. Flenner, J. Das, M. C. Rheinstädter, and I. Kosztin, *Phys. Rev. E* **79**, 011907 (2009).
- [24] C. L. Armstrong, M. Trapp, J. Peters, T. Seydel, and M. C. Rheinstädter, *Soft Matter* **7**, 8358 (2011).
- [25] W. L. C. Vaz, R. M. Clegg, and D. Hallman, *Biochem. J.* **24**, 781 (1985).
- [26] P. F. F. Almeida, W. L. C. Vaz, and T. E. Thompson, *Biochem. J.* **31**, 6739 (1992).
- [27] W. L. C. Vaz and P. F. Almeida, *Biophys. J.* **60**, 1553 (1991).
- [28] E. Falck, T. Róg, M. Karttunen, and I. Vattulainen, *J. Am. Chem. Soc.* **130**, 44 (2008).
- [29] S. Busch, C. Smuda, L. C. Pardo, and T. Unruh, *J. Am. Chem. Soc.* **132**, 3232 (2010).
- [30] G. R. Kneller, K. Baczynski, and M. Pasenkiewicz-Gierula, *J. Chem. Phys.* **135**, 141105 (2011).
- [31] T. Akimoto, E. Yamamoto, K. Yasuoka, Y. Hirano, and M. Yasui, *Phys. Rev. Lett.* **107**, 178103 (2011).
- [32] See Supplemental Material at <http://link.aps.org/supplemental/10.1103/PhysRevLett.109.188103> for additional figures and mathematical analyses.
- [33] Their chemical notation is 1, 2-distearoyl-*sn*-glycero-3-phosphatidylcholine (DSPC), 1,2-dioleoyl-*sn*-glycero-3-phosphatidylcholine (DOPC), and 1-stearoyl-2-oleoyl-*sn*-glycero-3-phosphatidylcholine (SOPC).
- [34] C. Hofstätter, E. Lindahl, and O. Edholm, *Biophys. J.* **84**, 2192 (2003).
- [35] H. Martinez-Seara, T. Róg, M. Pasenkiewicz-Gierula, I. Vattulainen, M. Karttunen, and R. Reigada, *Biophys. J.* **95**, 3295 (2008).
- [36] S. Burov, R. Metzler, and E. Barkai, *Proc. Natl. Acad. Sci. U.S.A.* **107**, 13228 (2010).
- [37] Free CTRW and FLE motions refer to the processes in free space, without external confining potential or obstacles that could constrain the motion.
- [38] Y. He, S. Burov, R. Metzler, and E. Barkai, *Phys. Rev. Lett.* **101**, 058101 (2008).
- [39] W. Deng and E. Barkai, *Phys. Rev. E* **79**, 011112 (2009).
- [40] J.-H. Jeon and R. Metzler, *Phys. Rev. E* **81**, 021103 (2010); **85**, 021147 (2012).
- [41] V. Tejedor, O. Bénichou, R. Voituriez, R. Jungmann, F. Simmel, C. Selhuber-Unkel, L. B. Oddershede, and R. Metzler, *Biophys. J.* **98**, 1364 (2010).
- [42] J.-H. Jeon and R. Metzler, *J. Phys. A* **43**, 252001 (2010).
- [43] H. Martinez-Seara, T. Róg, M. Karttunen, I. Vattulainen, R. Reigada, and N. Vij, *PLoS ONE* **5**, e11162 (2010).
- [44] M. R. Horton, F. Höfling, J. O. Rädler, and T. Franosch, *Soft Matter* **6**, 2648 (2010).
- [45] M. Javanainen, H. Hammaren, L. Monticelli, J.-H. Jeon, M. S. Miettinen, H. Martinez-Seara, R. Metzler, and I. Vattulainen, *Faraday Discuss.* (in press).
- [46] A. Filippov, G. Orådd, and G. Lindblom, *Biophys. J.* **84**, 3079 (2003).